Fracture toughness of low-pressure chemical-vapor-deposited polycrystalline silicon carbide thin films

V. Hatty and H. Kahn[a)]
Department of Materials Science and Engineering, Case Western Reserve University, 10900 Euclid Avenue, Cleveland, Ohio 44106

J. Trevino, C. A. Zorman, and M. Mehregany
Department of Electrical Engineering and Computer Science, Case Western Reserve University, 10900 Euclid Avenue, Cleveland, Ohio 44106

R. Ballarini
Department of Civil Engineering, Case Western Reserve University, 10900 Euclid Avenue, Cleveland, Ohio 44106

A. H. Heuer[b)]
Department of Materials Science and Engineering, Case Western Reserve University, 10900 Euclid Avenue, Cleveland, Ohio 44106

(Received 6 July 2005; accepted 21 November 2005; published online 12 January 2006)

The fracture toughness of thin-film polycrystalline silicon carbide (poly-SiC) deposited on silicon (Si) wafers via low-pressure chemical-vapor deposition (LPCVD) has been measured on a scale useful for micromachined devices; the results are compared to previous studies on poly-SiC thin films deposited by atmospheric pressure chemical-vapor deposition (APCVD) [Bellante *et al.*, Appl. Phys. Lett. **86**, 071920 (2005)]. Samples in this study included those with and without silicon dioxide (SiO_2) sacrificial release layers. The LPCVD processing technique induces residual tensile stresses in the films. Doubly clamped microtensile specimens were fabricated using standard micromachining processes, and microindentation was used to initiate atomically sharp precracks. The residual stresses in the films create stress intensity factors K at the crack tips; upon release, the precracks whose K exceeded a critical value, K_{IC}, propagated to failure. The fracture toughness K_{IC} was the same for both types of devices, 2.9 ± 0.2 MPa $m^{1/2}$ for the SiC on Si samples and 3.0 ± 0.2 MPa $m^{1/2}$ for the SiC on SiO_2/Si samples, and similar to that found for APCVD poly-SiC, $2.8 \leqslant K_{IC} \leqslant 3.4$ MPa $m^{1/2}$ [Bellante *et al.*, Appl. Phys. Lett. **86**, 071920 (2005)], indicating that K_{IC} is truly a structure-insensitive material property. The fracture toughness of poly-SiC compares favorably with that for polysilicon, 0.85 ± 0.05 MPa $m^{1/2}$ [Kahn *et al.*, Science **298**, 1215 (2002)]. © *2006 American Institute of Physics*. [DOI: 10.1063/1.2158135]

I. INTRODUCTION

Silicon carbide (SiC) is receiving increasing attention as a structural material in microelectromechanical systems (MEMS), due to its outstanding properties.[1,2] In addition to its excellent mechanical, chemical, and thermal properties that enable MEMS devices to operate under harsh environments and in demanding applications, SiC semiconductor technology also enables high-temperature and radiation-resistant electronics due to the wide band gap, 2.3–3.4 eV, depending on polytype.[2] As a result, SiC sensors and actuators can be deployed in applications where silicon technology would not be practical (e.g., instrumentation and control in power generation, propulsion, deep space, and resource exploration systems, to name a few).

Intrinsic material properties, i.e., those independent of specimen geometry, impact the lifetimes of MEMS devices,[3] and it is important to know whether the behavior of thin films of a certain material differs dramatically from its bulk counterpart. An important material property is fracture toughness K_{IC}, the intrinsic ability of a material to withstand crack propagation. We previously reported K_{IC} of atmospheric pressure chemical-vapor deposition (APCVD) poly-SiC deposited on Si.[4] In the present work, we compare those results to K_{IC} of low-pressure chemical-vapor deposition (LPCVD) poly-SiC deposited on both Si and SiO_2. The fracture toughness does not appear to depend on deposition conditions, substrate, or size and can truly be considered a structure-insensitive property. This material is associated with a vanishingly small crack-tip process zone, as implied by the fact that the measured K_{IC} is similar to that of a bulk sample.[5] We have previously reported[6] similar structure insensitivity of K_{IC} for polysilicon. Furthermore, the atomic force microscopy (AFM) results of Chasiotis *et al.* show that the crack-tip fields in polysilicon structures with characteristic dimensions of the order of tens of microns are well predicted by linear elastic fracture mechanics[7,8] and therefore do not exhibit any size effects.

II. EXPERIMENTAL PROCEDURES

To determine K_{IC} in LPCVD SiC thin films, we utilized a fixed grip, fixed displacement tensile test using precracked

[a)]Electronic mail: harold.kahn@case.edu
[b)]Electronic mail: arthur.heuer@case.edu

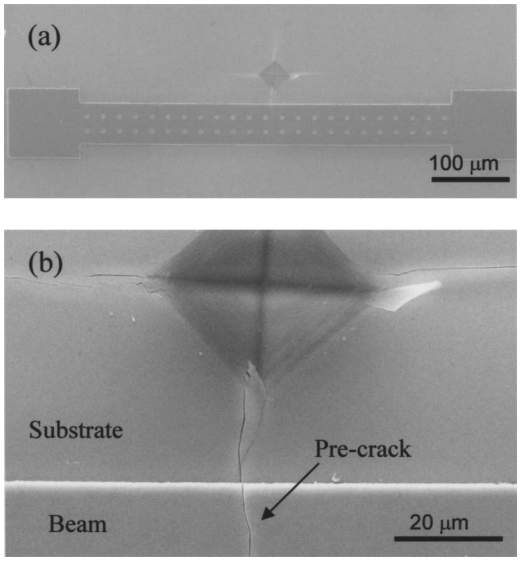

FIG. 1. (a) SEM micrograph of a 500×60 μm^1 doubly clamped microtensile specimen and the location of a Vickers indent. (b) Higher magnification SEM micrograph of the Si substrate and the propagation of the precrack into the poly-SiC beam.

specimens under constant (residual) growth stress.[4,6] We fabricated doubly clamped microtensile beams, 60 μm wide and 500 μm long, introduced a single atomically sharp edge crack, and used the residual tensile stresses in the beam to load the cracks and determine the fracture toughness of the SiC film. (The cracks large enough to have K at the crack tips $>K_{IC}$ propagated to failure during release—see below.)

Specimens were fabricated as follows: nitrogen-doped poly-SiC was deposited onto 100-mm-diameter (100) Si wafers at 900 °C using SiH_2Cl_2 and C_2H_2 as the Si and C precursors and NH_3 as the dopant source gas.[9] The nominal thickness of the films was 800 nm. Standard photolithography processes were used to pattern the microtensile devices. Each microtensile specimen was fabricated with 2×2 μm^2 etch holes spaced 20 μm apart, as shown in Fig. 1(a), to aid the release process. Half of the specimens in this study had a thermally grown oxide layer between the (100) Si and poly-SiC. 10×10 mm^2 dies from 16 wafers were tested. From each die, ten microtensile beams were tested. The film stress was determined using wafer curvature measurements. A total of 160 edge-cracked, doubly clamped microtensile specimens were indented and released.

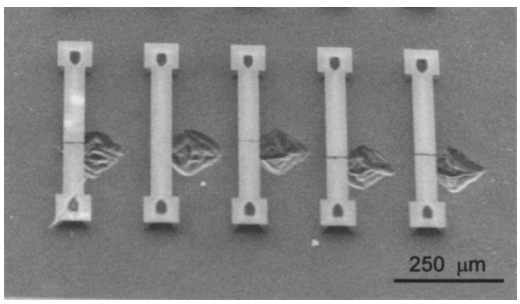

FIG. 2. SEM micrograph of the microtensile specimens after Vickers microindentation and timed aqueous etching. Precracks in four of the beams propagated upon release; the beam second from the left remained intact.

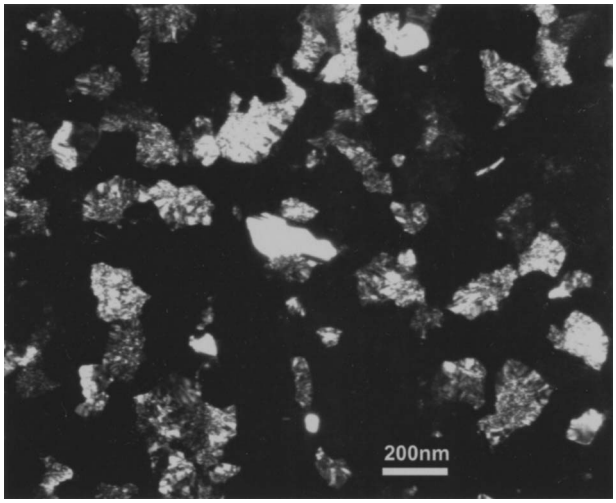

FIG. 3. Plan view, dark field transmission electron micrograph of the LPCVD poly-SiC thin film used in this study grown on Si. The microstructure shows an average grain diameter of 100 nm. No Si inclusions or voids are present in the poly-SiC film.

As shown in Fig. 1, the substrate was indented by a Vickers microindent near each beam with a 1 kg load to initiate atomically sharp precracks that propagated through the Si substrate and into the poly-SiC doubly clamped beams. Sharp precracks were thus initiated in the beam, and the damage associated with indentation was restricted to the substrate; no detectable displacement of the anchor pads occurred. However, to ensure that the anchors at the ends of each beam did not deflect in a manner that could affect the stress intensity factor calculations, the compliance of each anchor was estimated. The Appendix includes a rigorous calculation that demonstrates that upon release, the stress in the film remained constant, and no error was introduced into the stress intensity factor calculation. The anchor pads at both ends of the beams remained firmly attached to the substrate upon release, due to their large lateral dimensions.

Precrack lengths were measured with a scanning electron microscope (SEM). The beams were released by a timed aqueous etch; the SiC on Si specimens were etched for approximately 2 min with a 1:2:2 solution of $HF(49\%):HNO_3(69\%):CH_3COOH(100\%)$ and the SiC on SiO_2/Si specimens were etched for 5 min with an aqueous

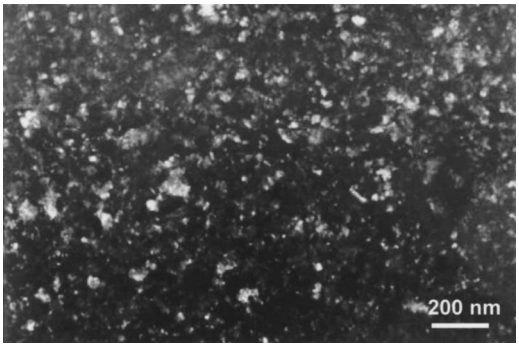

FIG. 4. Plan view, dark field transmission electron micrograph of APCVD poly-SiC thin film grown on Si used in previous work (see Ref. 4). The grain size is smaller than that of LPCVD poly-Si thin film used in the present study.

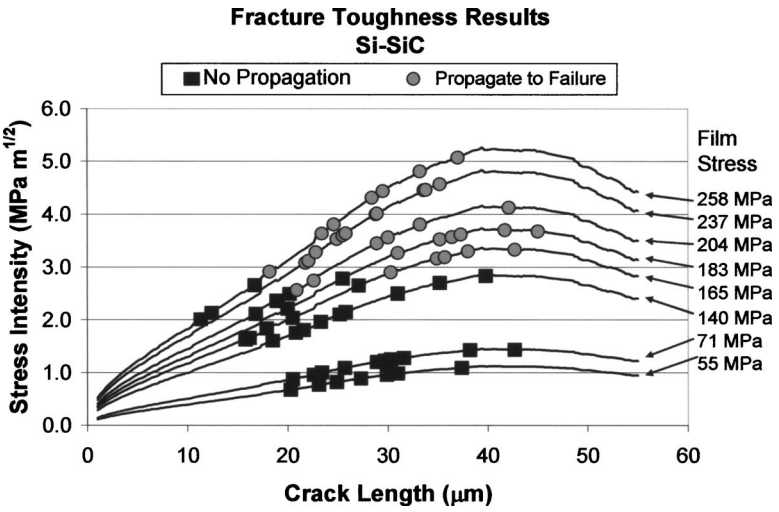

FIG. 5. Stress intensity factor calculated with finite element analysis vs crack length for poly-SiC on Si specimens with failed and intact data points shown as circles and squares, respectively.

HF(49%) solution. The residual stress in the film caused a well-defined stress intensity at the crack tip. As noted above, upon release of the microtensile specimens, crack growth occurred from precracks whose stress intensity factor K was greater than K_{IC}, whereas growth did not occur for precracks whose K was lower than K_{IC}. Due to the range of residual stresses and precrack lengths, a range of stress intensities were produced. Figure 2 is a SEM image of five microtensile specimens after release. The precracks in four of the beams propagated upon release; the beam second from the left remained intact.

Figure 3 is a plan view, dark field transmission electron micrograph of the SiC LPCVD film and shows that the microstructure is characterized by an average grain diameter of 100 nm and is free of Si inclusions and/or voids. The 3*C*-SiC film has a $\langle 110 \rangle$ texture.[9] Figure 4 is a plan view, dark field transmission electron micrograph of the APCVD SiC film tested previously, which is essentially untextured.[10] The microstructure of this material (Fig. 4) is characterized by a smaller grain size than the LPCVD SiC film, ~20 nm. In both types of films, the small grain size ensures that the precrack front passes through several grains with varying orientations, and therefore no effect due to a possible crystallographic anisotropy of fracture toughness is expected.

III. RESULTS AND DISCUSSION

The residual stresses from each wafer varied from 51 to 258 MPa. Figures 5 and 6 show the stress intensity as a function of precrack length prior to release, as determined by finite element analysis,[11] for both SiC on Si specimens and SiC on SiO_2/Si specimens. The K vs precrack length curves show a maximum value due to the geometry of the specimen.[12] Failed and intact data are shown as circles and squares, respectively. The critical stress intensity K_{IC} is bounded between the lowest K that caused propagation and the highest K that did not. K_{IC} data were essentially identical for the two types of specimen: 2.9 ± 0.2 MPa $m^{1/2}$ for SiC on Si samples and 3.0 ± 0.2 MPa $m^{1/2}$ for SiC on SiO_2/Si samples.

We have assumed perfectly straight precracks with straight crack fronts in our analysis, perpendicular to the beam axes, and it is necessary to examine this assumption. The fracture surface of one beam that suffered catastrophic crack propagation upon release is shown in Fig. 7. As can be seen, the precrack front has curved through the thickness of the beam from the bottom to the top surface, and the variation in precrack length through the beam thickness could be as large as 1 μm. The precrack length measurements using

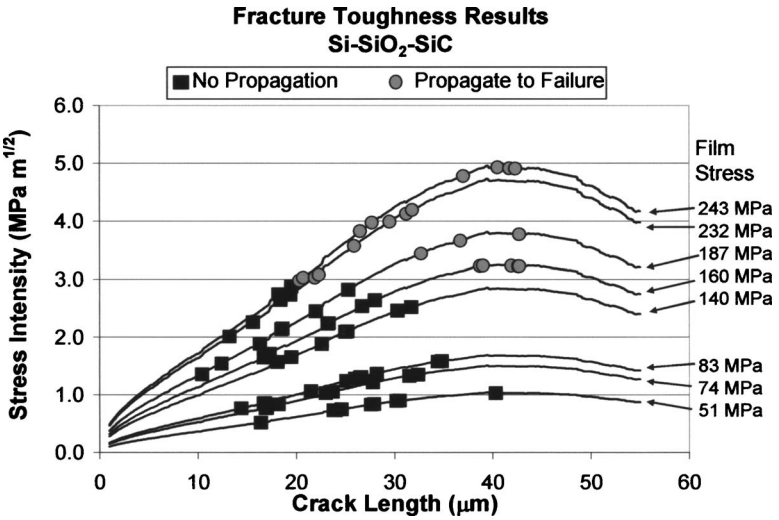

FIG. 6. Stress intensity factor calculated with finite element analysis vs crack length for SiC on SiO_2/Si specimens with failed and intact data points shown as circles and squares, respectively.

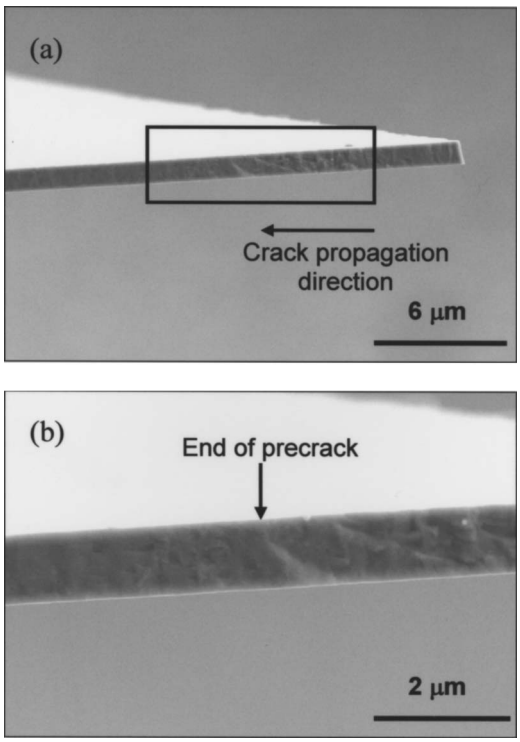

FIG. 7. SEM micrographs of the fracture surface (a) from a microtensile specimen and (b) higher magnification of the transition of a precrack which propagated to failure due to residual stresses in the film.

the SEM actually determined the precrack length at the top surface, and this uncertainty does lead to potential errors in the determination of K_{IC}. However, these are not thought to be greater than 10%.

In addition, and although scatter in the data is not large, there are residual stress variations throughout each die, which we neglect, as well as neglect of the etch holes, which in the finite element analysis represent 0.6% of the total area of the microtensile specimen. Both factors are thought to be less important than the ±10% uncertainty in precrack length.

In a previous study on APCVD poly-SiC, we determined $2.8 \leqslant K_{IC} \leqslant 3.4$ MPa $m^{1/2}$. The similar K_{IC} values reported here for the different deposition techniques are consistent with our theoretical understanding that K_{IC} is an intrinsic material property of a brittle material and independent of the microstructure of poly-SiC. Finally, K_{IC} for polysilicon is 0.85 ± 0.05 MPa $m^{1/2}$.[6] For equivalent flaw sizes, say, those introduced by plasma etching during device fabrication, poly-SiC can withstand loads three times higher than polysilicon without failure.

IV. CONCLUSION

Critical stress intensity factors of heavily N-doped poly-SiC, deposited by LPCVD, were measured on 160 microtensile specimens fabricated using processes and size scales relevant to MEMS devices. We utilized a fixed grip, fixed displacement tensile test using precracked specimen under constant (residual) stress. Doubly clamped microtensile beams were fabricated and indented to introduce a single atomically sharp edge crack. The residual tensile stresses in the beam loaded the precracks in such a way that allowed the fracture toughness of the SiC film to be determined. Stress intensities at the crack tip that exceeded a critical value K_{IC} propagated to failure upon release. K_{IC} data were essentially identical for the two types of specimen: 2.9 ± 0.2 MPa $m^{1/2}$ for SiC on Si samples and 3.0 ± 0.2 MPa $m^{1/2}$ for SiC on SiO_2/Si samples, and similar to the data for APCVD material $2.8 \leqslant K_{IC} \leqslant 3.4$ MPa $m^{1/2}$.

ACKNOWLEDGMENTS

The authors thank Dr. Glenn Beheim of NASA Glenn Research Center for etching the SiC films. This research was funded in part by a grant from the National Science Foundation (ECS-0327674). The authors thank Dr. Ming Zhang for providing the TEM micrograph of the LPCVD SiC film and Dr. Chien-Hung Wu for the TEM micrograph of the APCVD film.

APPENDIX

To ensure that the anchors at the ends of each beam did not displace sufficiently after release to affect the stress intensity factor calculations, the deformation of each anchor was estimated as follows. The linear expansion of the film δ_F upon release is given by

$$\delta_F = \frac{\sigma_R L}{E_{SiC}} - \frac{FL}{E_{SiC} A_{beam}}, \tag{A1}$$

where the first term is the free expansion and the second term is due to the constraining force F by the anchors. σ_R is the residual stress in the film measured from wafer curvature methods, L is the length of the SiC beam, and E_{SiC} is the elastic modulus of SiC.

For SiO_2 release layers, the anchor is assumed to be a square SiO_2 pillar, 2 μm high and 40 μm wide. Since the height of the anchor is small in comparison to its cross-sectional area, it is assumed that the shear stress, τ, is zero through the thickness of the anchor, and the displacement of the anchor δ_A is given by

$$\delta_A = \frac{F h_A}{A_A G_A}, \tag{A2}$$

where h_A is the height of the anchor, A_A is the cross-sectional area of the anchor, and G_A is the shear modulus of the anchor. Compatibility demands that $\delta_A = \delta_F$. This provides the force in the film

$$F = \frac{\sigma_R L / E_{SiC}}{(h_A / A_A G_A + L / E_{SiC} A_{beam})} \tag{A3}$$

and the stress in the film after release, which is given by

$$\sigma_F = \frac{F}{A_{beam}}. \tag{A4}$$

The dimensions of the SiC beam are 500 μm in length, 60 μm in width, and 0.7 μm in thickness. The elastic modulus of SiC E_{SiC} is 440 GPa.[13] Since $E_{SiO_2} = 72$ GPa and $\nu_{SiO_2} = 0.16$,[14] the shear modulus, G_{SiO_2}, is 31 GPa. For the highest measured residual stress, $\sigma_R = 258$ MPa, $F = 1.08 \times 10^{-2}$ N, and the stress in the film after release is σ_F

=257 MPa. The correction in film stress is negligible in the stress intensity factor calculations.

Without the SiO_2 release layer, the anchor is assumed to be a square Si pillar, 30 μm high and 40 μm wide. This geometry does not fit either of the limiting cases: the shear analysis discussed above or a slender cantilever beam where the height $h_A \gg$ the width w. Therefore, we will conduct both analyses and treat them as worst-case scenarios. This is especially true for the cantilever beam assumption, since the top surface of the actual anchor is constrained by the SiC beam to remain parallel to the substrate, which will limit its deflection. The shear modulus of Si on the {100} plane in the [110] direction is 50 GPa, and the elastic modulus E_{Si} =170 GPa.[15] For the slender cantilever beam approximation, the displacement of the anchor is

$$\delta_A = \frac{Fh^3}{3E_{Si}I} = \frac{4Fh^3}{E_{Si}w^4}, \tag{A5}$$

where I is the moment of inertia of the (square cross-sectional) cantilever. The force in the film determined from the compatibility relationship is given by

$$F = \frac{\sigma_R L/E_{SiC}}{(4h_A^3/E_{Si}w^4 + L/E_{SiC}A_{beam})}. \tag{A6}$$

Using the values given above, $F=1.074\times10^{-2}$ N and the stress in the film after release σ_F=256 MPa. For the other limiting case, using Eqs. (A1)–(A4) given above, the force in the film after release is $F=1.067\times10^{-2}$ N and σ_F =254 MPa. The difference in stress after release bounded by the two extreme cases is 0.8%–1.5%. From the graphs in Figs. 5 and 6 it is clear that this small change in stress has a negligible effect on the stress intensity factor calculations. Thus, it can be assumed that the ends of the beams remained firmly in place upon release due to their large lateral dimensions of the anchors.

[1] M. Mehregany and C. A. Zorman, Thin Solid Films **355–366**, 518 (1999).
[2] G. L. Harris, *Properties of Silicon Carbide* (INSPEC, London, 1995).
[3] A. D. Romig, Jr., M. T. Dugger, and P. J. McWhorter, Acta Mater. **51**, 5837 (2003).
[4] J. J. Bellante, H. Kahn, R. Ballarini, C. A. Zorman, M. Mehregany, and A. H. Heuer, Appl. Phys. Lett. **86**, 071920 (2005).
[5] http://www.ceramics.nist.gov/srd/summary/scdscs.htm
[6] H. Kahn, R. Ballarini, J. J. Ballante, and A. H. Heuer, Science **298**, 1215 (2002).
[7] I. Chasiotis, S. W. Cho, and K. Jonnalagadda, J. Appl. Mech. (to be published).
[8] I. Chasiotis, S. W. Cho, and K. Jonnalagadda, *Proceedings of the Materials Research Society 854E*, 2005 (electronic publication), pp. U.10.6.1–U.10.6.6.
[9] J. Trevino, X.-A. Fu, M. Mehregany, and C. Zorman, *Proceedings of the 18th IEEE International Conference on Micro-Electro-Mechanical Systems*, Miami, FL, 30 January–3 February 2005 (unpublished), pp. 451–454.
[10] C. H. Wu, Ph.D. dissertation, Case Western Reserve University, 2001.
[11] The finite element code FRANC 2D was used to determine stress intensities. This code is available from the Cornell Fracture Group at http://www.Cfg.cornaell.edu/
[12] H. Tada, P. C. Paris, and G. R. Irwin, *The Stress Analysis of Cracks Handbook* (American Society of Mechanical Engineers, New York, 2000).
[13] M. W. Barsoum, *Fundamentals of Ceramics* (Institute of Physics, Philadelphia, PA, 2003).
[14] S. D. Senturia, *Microsystem Design* (Kluwer Academic, Boston, 2001).
[15] J. J. Wortman and R. A. Evans, J. Appl. Phys. **36**, 153 (1963).